A Planar Structure Sensitive to Out-of-plane Forces for the Force-controlled Injection of Suspended and Adherent Cells

Denis Desmaële, Mehdi Boukallel and Stéphane Régnier

***Abstract*— We present a novel force sensor for the injection of both suspended and adherent cells. Unlike most configurations, this force sensor is independent of the tool interacting with the cells. It is a planar structure that provides a surface sensitive to out-of-plane forces where living cells can be placed for manipulation. It also integrates two beam resonators. Forces perpendicular to the sensor's plane are estimated via frequency shifts of the resonators. In this paper, we develop a theoretical study for predicting and optimizing the structure's sensitivity. As a proof of concept, we report the fabrication and characterization of a first prototype designed for the injection of spherical cells with a diameter of ∼100-600 μm. In air, our prototype presently offers a quality factor of 700, and a linear force sensitivity of ∼2.6 Hz/mN. The measurement of forces applied upon lobster eggs is also experimentally demonstrated.**

I. INTRODUCTION

The possibility to safely inject small volumes of foreign compounds into living cells plays a prominent role in many life sciences such as genetics, transgenics, molecular biology or drug discovery.

During the penetration of the cellular membrane, it is necessary to estimate the interaction force between the cell and the injection micropipette. Indeed, cells are prone to irremediable damages if excessive forces are applied during the injection process. Hence, to ensure higher success and survival rates, cell injection systems must be equipped with force measurement systems in order to implement force control.

To date, most cell injection systems have been designed to inject spherical suspended cells (e.g., embryos, oocytes). To estimate the force applied upon such cells, vision-based techniques that track cell deformations can be used. However, to recover the force solely from visual feedback, the elastic properties of the cell to be injected must usually be known *a priori* [1]. Moreover, the resolution of vision-based techniques is inherently limited by the optical components of the microscope. Therefore, the use of an additional *contact-based* force sensor is usually preferred.

Conventionally, for measuring the penetration force of embryos or oocytes, an injection micropipette is bonded to the free end of a compliant cantilever covered with sensitive films (e.g., [2], [3]). The pressure tube which is connected to the micropipette for the delivery of liquid samples can however affect the penetration force measurement [4]. In addition, the sensitive cantilever bends during the penetration phase. Compared to a rigid glass micropipette, this bending can cause more puncture damages to the cell [4].

Other types of force sensors (e.g., [5], [6]) circumvent the drawbacks inherent to cantilevered micropipettes, but only for suspended cells. To the best of the authors' knowledge, the force-controlled injection of adherent cells with irregular morphology (e.g., mammalian cells such a fibroblasts, HeLa cells, endothelial cells) has only been recently reported in [7]. Nonetheless, the force sensitive setup is based on an expensive atomic force microscope.

We therefore find that the capability to measure cell penetration forces for different types of cells in a cost-effective manner remains challenging. In this paper, we propose a novel type of force sensor designed to bring new solutions to this problem. Ultimately, this force sensor could target both adherent and suspended cells whereas low-cost and commercially available glass micropipettes can be used during the injection process.

II. SENSOR DESCRIPTION AND WORKING PRINCIPLE

The proposed force sensor acts as a cell substrate sensitive to out-of-plane (perpendicular) forces. As depicted in Fig.1, it is a monolithic structure that exploits a specific vibration mode where two beam resonators (outer beams) oscillate in antiphase, whereas a third beam (central beam) remains immovable.

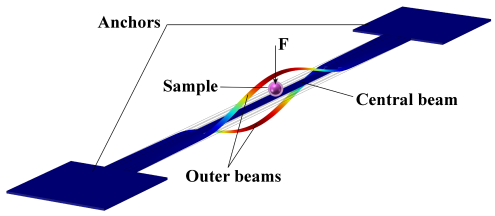

Fig. 1. Concept of the force sensitive cell substrate illustrated with a suspended cell (trapping system for maintaining the cell not represented). To measure the injection force F imposed to the cell, a vibration mode where two outer beams oscillate in antiphase is exploited. The cell is placed on a third central beam which remains immovable.

Thereby, the area located at the half span of the central steady beam can be used to place and inject cells. One can envision to coat this location with biochemicals to culture and inject a few adherent cells. Alternatively, a trapping system can be implemented to grab and hold suspended cells.

D. Desmaële and M. Boukallel are with the CEA, LIST, Sensory and Ambient Interfaces Laboratory, 18 Route du Panorama, BP6, Fontenay-aux-Roses, F-92265, France; denis.desmaele@cea.fr, mehdi.boukallel@cea.fr

Stéphane Régnier is with the Institut des Systèmes Intelligents et de Robotique, Université Pierre et Marie Curie, CNRS - UMR 7222, 4 Place Jussieu, 75252, Paris Cedex 05, France; stephane.regnier@upmc.fr

Since this force sensor is independent of the tool interacting with the cells, conventional glass micropipettes can be used for the delivery of foreign compounds. During the injection process, if the force F generated by the micropipette is applied perpendicular to the structure's plane, the whole structure deflects. In fact, even a slight static deflection imposed by F impacts the resonators' dynamics and affects their operation frequency. Accordingly, it is possible to recover the magnitude of the normal force applied upon the cells by monitoring frequency shifts of the outer beams.

III. THEORETICAL ANALYSIS

A. Large deflections of the planar structure

To predict frequency shifts engendered by a normal force F applied to the central beam, static and dynamic behaviors are studied independently. The static analysis is first conducted in order to detail how the outer beams exactly behave during the deflection of the whole structure. Due to symmetry, our analysis can be limited to one fourth of the structure (see Fig.2).

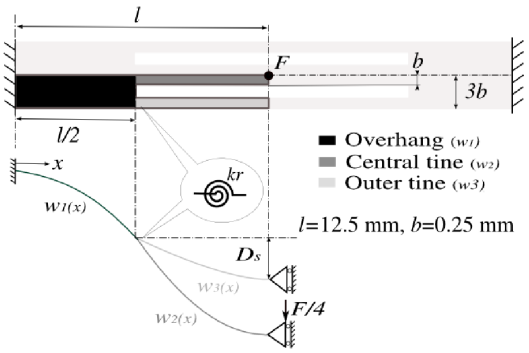

Fig. 2. Top: for predicting the quasi-static deflection of the structure, only the darker *"tuning fork"* (top view) is considered. Bottom: equivalent one-dimensional model (side view) of the colored beams (proportions exaggerated for illustration purposes).

This quarter structure, similar in shape to a tuning fork, is composed of three segments. All segments are assumed to satisfy Bernouilli's beam theory. One-dimensional coordinate functions are used to approximate the displacement field of each segment. Considering a set of geometrical and mechanical constraints, we can choose to model the flexural displacement $w_{1,2,3}(x)$ of each segment by second order polynomial expressions

$$\begin{cases} w_1(x) = a_2\, x^2 \\ w_2(x) = \dfrac{a_2}{2}\left(-2x^2 + 4lx - l^2\right) \\ w_3(x) = \dfrac{a_2}{4}\left[l^2 - \dfrac{6lk_r\,(4x^2 - 8lx + 3l^2)}{6lk_r + Ebh^3}\right] \end{cases} \tag{1}$$

where l and b are defined in Fig.2, $E = 212$ GPa is the Young's modulus, $h = 0.1$ mm is the structure's thickness, a_2 is a free unknown parameter, and $k_r = 0.7 \times 10^{-3}$ Nm/rd represents the rotational stiffness that links the outer tine to the overhang at $x = l/2$.

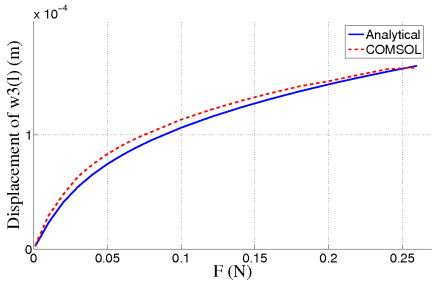

Fig. 3. Half span deflection of an *outer* beam for a normal force F applied to the *central* beam.

With (1), we use an energy approach to derive the relationship governing the maximum displacement of the outer tine when the force F is applied at the extremity of the central tine. During deflection, the potential energy stored by the tuning fork is $U_{tf} = U_b + U_s$, where U_b is the sum of strain energies developed by each segment during bending

$$U_b = \sum_{i=1}^{3} \frac{1}{2}\, EI_i \int_0^{l/2} \left(\frac{d^2 w_i}{dx^2}\right)^2 dx. \tag{2}$$

In (2), $I_1 = bh^3/4$ and $I_2 = I_3 = bh^3/12$.

Similarly, U_s is the sum of energy contributions due to the axial stretching of the segments

$$U_s = \sum_{j=1}^{3} \frac{EA_j}{4l} \left[\int_{c_j}^{d_j} \left(\frac{dw_j}{dx}\right)^2 dx\right]^2 \tag{3}$$

where $c_1 = 0$, $d_1 = l/2$, $c_{2,3} = l/2$ and $d_{2,3} = l$. A_j in (3) represents the cross section areas of the three segments with $A_1 = 3bh$ and $A_{2,3} = bh$. By considering the work $W = Fw_2(l)$ done by the punctual force F, the unknown parameter a_2 in (1) can be simply found by minimizing the total potential energy function $\Phi = U_{tf} - W$.

Fig.3 compares our static modeling approach to finite element analysis (FEA) simulations for predicting the half span deflection of an outer beam. As it can be observed, the stretching effect progressively dominates as the outer beam deflection increases above ~50% of the structure's thickness.

B. Frequency variations of pre-bent outer beams

A dynamic analysis can now be carried out in order to predict how the static deflection imposed by F to the outer beams impacts their initial resonance frequency. Since we are only interested in the antisymmetrical vibration mode illustrated in Fig.1, we can actually grasp valuable insights on the structure's dynamics by restricting our study to a single outer beam (see Fig.4).

To a first approximation, we assume that the outer beam can be modeled as a hinged-hinged beam terminated by two rotational springs of stiffness $k_{r_1} = 10.5 \times 10^{-3}$ Nm/rd For such boundary conditions, it is conventional to assume a displacement function in the form of a sine $w(x) = D_s \sin(\pi x/l)$, where D_s is the half span deflection of the beam (see Fig.4).

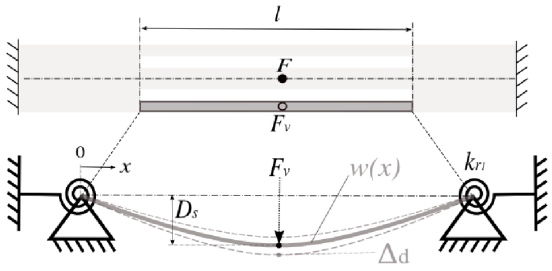

Fig. 4. For predicting frequency shifts, only one outer beam is considered. Vibrations Δ_d (dashed gray lines) take place around an equilibrium position D_s (thick gray line). The curved profile $w(x)$ is indirectly engendered by static deflections imposed by F (proportions exaggerated for illustration purposes).

As depicted in Fig.2, $D_s = w_3(l) - w_1(l/2)$ is related to the force F applied to the central steady beam. Conceptually, it is however more convenient to consider that D_s is rather due to an unknown virtual force F_v directly applied at $w(l/2)$ (see Fig.4). With an energy approach, a *cubic force-centered-deflection law* between D_s and F_v can be derived

$$F_v = \left(\frac{Ebh^3\pi^4}{24l^3} + \frac{2k_{r_1}\pi^2}{l^2} \right) D_s + \frac{Ebh\pi^4}{8l^3} D_s^3. \quad (4)$$

We then assume that small deflections of the beam about a mean deflection D_s can be described approximately by a single stiffness value. Considering that vibration amplitudes Δ_d (see Fig. 4) are sufficiently small, the equivalent stiffness of the outer beam may be approximated by

$$k_{eq} = \frac{dF_v}{d\Delta_d} \approx \left(\frac{Ebh^3\pi^4}{24l^3} + \frac{2k_{r_1}\pi^2}{l^2} \right) + \frac{3Ebh\pi^4}{8l^3} D_s^2. \quad (5)$$

If we consider to a first approximation that our single outer beam oscillates as an undamped lumped-parameter system, the static deflection D_s affects its natural frequency f_0 as follows

$$\frac{f}{f_0} \approx \sqrt{1 + \frac{9Ebh\pi^2 D_s^2}{Ebh^3\pi^2 + 48lk_{r_1}}}. \quad (6)$$

Despite the fact that (6) only considers one outer beam with approximate boundary conditions, Fig.5 shows that frequency variations predicted by (6) are in accordance with FEA results.

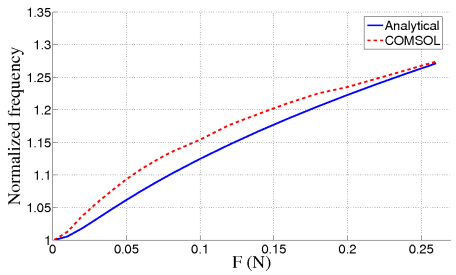

Fig. 5. Frequency shift of the outer beams predicted when a normal force F is imposed upon the central beam.

IV. EXPERIMENTAL VALIDATION

As a proof of concept, we fabricated a first experimental prototype intended to the injection of cells whose diameter approximately ranges from 100 to 600 μm (see Fig.6). This monolithic prototype was fabricated from a single sheet of biocompatible stainless steel using wire cut electric discharge machining. All dimensions are those used for the theoretical analysis. Mechanical excitation was provided by a 3 mm long, 2 mm wide and 200 μm thick piezoelectric (PZT) element (Physik Instrumente PIC151) bonded onto the structure. To monitor the operating frequency of the oscillating outer beams, we implemented a microscopic optical fiber probe similar to the one reported in [8].

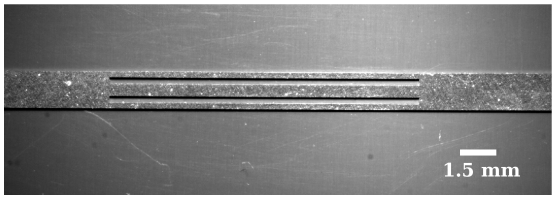

Fig. 6. Close-up of the experimental prototype manufactured (PZT element not visible).

A. Experimental characterization of the prototype

For characterizing the prototype, we first evaluated some of its intrinsic performances with no force applied to the central beam. The antisymmetrical mode of Fig.1 was found when driving the PZT element around 3180 Hz. When the PZT was voltage supplied with a peak-peak AC signal of 9 V, the maximum oscillation amplitude of the outer beams was 11 μm. Potential vibrations at the half span of the central beam were checked. They never exceeded 400 nm, namely 2% of the outer beams oscillation amplitude. In addition, we explored the frequency response of the antisymmetrical mode. In ambient conditions (i.e., in air), a quality factor of $\sim$700 was obtained (Fig.7).

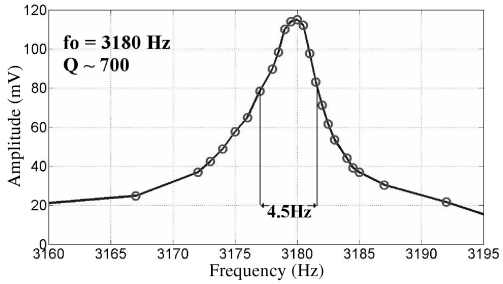

Fig. 7. Blown-up of the frequency response for the antisymmetrical mode of vibrations of Fig.1.

To apply a force perpendicular to the central beam, we used an indenter whose vertical position was controlled by a micropositioning stage (Physik Instrumente M112-1DG). This indenter was terminated by a metal bead whose diameter was approximately 500 μm. The bead's stiffness was much higher than the prototype's stiffness. To estimate the

force F applied to the central beam during displacements, we characterized our indenter. By translating the indenter against a precision electrical scale (Kern 440-33), a linear relationship was found for a displacement d ranging from 0 to 300 μm (data not shown)

$$F \approx 2201.4\, d - 0.001. \tag{7}$$

We then bent the central beam with the indenter. For each displacement step applied (10 μm), drastic changes in the oscillation amplitude of the resonant outer beams occurred. These easily detectable amplitude changes permitted to recover frequency shifts [9].

As a result, we found that the frequency varied linearly with an increased force sensitivity when the deflection of the central beam reached 210 μm. Hence, we forced the central beam to stay permanently deflected at this position. In order to maintain this new static equilibrium, we applied a slight axial compression to the whole structure. Although the initial resonance frequency of the outer beams dropped, this axial compression did not significantly change the dynamic behavior of the prototype. As shown in Fig.9, this slightly curved configuration of our prototype provides a force sensitivity of $\sim$ 2.6 Hz/mN (solid line).

B. Force applied on lobster eggs

To demonstrate the possibility to use our force sensitive surface in cell injection tasks, we applied a force on lobster eggs. Nevertheless, since our current prototype does not include a system able to hold a suspended cell, lobster eggs were not directly placed on the central beam, as depicted in Fig.1. Instead, it was easier to remove the metal bead of our indenter and replace it by the lobster eggs. Eggs were sorted to have also an approximate diameter of 500 μm.

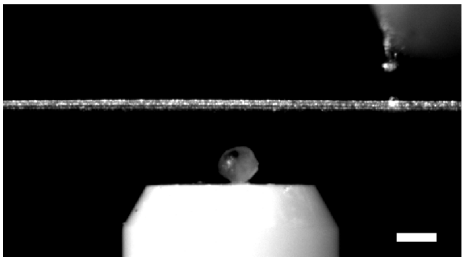

Fig. 8. Side view of the slightly curved prototype for measuring the force applied upon a lobster egg. The optical fiber probe used to monitor the resonance frequency of the outer beams is visible in the upper right corner. Scale bar represents 500 μm.

With the prototype slightly curved, the eggs were then gently pressed upon the central beam by translating the indenter. The frequency shift measured during the squeezing of one egg is shown in Fig.9 (dashed line). As it can be observed, a force up to 90 mN was applied to the egg. Such a force magnitude can be explained by the fact that we did not use a sharp tool able to puncture the egg membrane. Considering injection forces reported in [3] for flying fish egg cells, it is however demonstrated that our prototype would allow to measure penetration forces for cells of similar size.

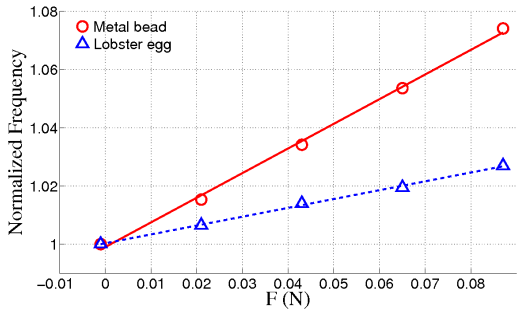

Fig. 9. Comparison of frequency shifts induced when applying a force F to the slightly curved central beam with the indenter terminated either by a metal bead or a lobster egg. $\triangle$ and O correspond to experimental measurements. Solid and dashed lines are fitted frequency shifts.

V. CONCLUSION AND FUTURE WORK

This paper has presented the design and fabrication of a novel type of force sensor intended to cell injection tasks. The sensor acts as a force sensitive substrate where adherent or suspended cells can be safely placed for manipulation. Moreover, low-cost glass micropipettes can be used since the sensor is independent of the tool interacting with the cells. A first prototype has been experimentally characterized. In particular, an encouraging force sensitivity of 2.6 Hz/mN has been reported. This force sensitivity allowed to measure forces applied on lobster eggs with a diameter of $\sim$500 μm. As a next step, the design and integration of a trapping system is currently investigated. Moreover, the miniaturization of the system for the injection of smaller cells is ongoing.

REFERENCES

[1] Y. Sun, B. J. Nelson, and M. Greminger, "Investigating protein structure change in the zona pellucida with a microrobotic system," *Int. J. Robot. Res.*, vol. 24, no. 2–3, pp. 211–218, 2005.

[2] D.-H. Kim, S. Yun, and B. Kim, "Mechanical force response of single living cells using microrobotic system," in *Int. Conf. on Robotics and Automation*, New Orleans, LA, April 2004, pp. 5013–5018.

[3] A. Pillarisetti, W. Anjum, J. P. Desai, G. Friedman, and A. D. Brooks, "Force feedback interface for cell injection," in *Joint Eurohaptics Conf. Symp. on Haptic Interfaces for Virtual Environment and Teleoperator Syst.*, Pisa, Italy, March 18-20, 2005, pp. 391–400.

[4] Y. Xie, D. Sun, and C. Liu, "Penetration force measurement and control in robotic cell microinjection," in *IEEE/RSJ Int. Conf. on Intelligent Robots and Syst.*, St. Louis, USA, October, 11-15, 2009, pp. 4701–4706.

[5] Y. Sun, K.-T. Wan, K. P. Roberts, J. C. Bischof, and B. J. Nelson, "Mechanical property characterization of mouse zona pellucida," *IEEE Trans. Nanobiosci.*, vol. 2, no. 4, pp. 279–286, 2003.

[6] X. Liu, Y. Sun, W. Wang, and B. Lansdorp, "Vision-based cellular force measurement using an elastic microfabricated device," *J. Micromech. Microeng.*, vol. 17, no. 7, pp. 1281–1288, 2007.

[7] A. Meister, M. Gabi, P. Behr, P. Studer, J. Vörös, P. Niedermann, J. Bitterli, J. Polesel-Maris, M. Liley, H. Heinzelmann, and T. Zambelli, "FluidFM: combining atomic force microscopy and nanofluidics in a universal delivery system for single cell applications and beyond," *Nano Lett.*, vol. 9, no. 6, pp. 2501–2507, 2009.

[8] G. Perrone and A. Vallan, "A low-cost optical sensor for noncontact vibration measurements," *IEEE Trans. Instrum. Meas.*, vol. 58, pp. 1650–1656, May 2009.

[9] K. Fukuzawa, T. Ando, M. Shibamoto, Y. Mitsuya, and H. Zhang, "Monolithically fabricated double-ended tuning fork based force sensor," *J. Appl. Phys.*, vol. 99, p. 094901 (5pp), 2006.